^{14}N NQR and Orientational Ordering in Smectic Liquid Crystals

R. Blinc, M. Vilfan and J. Seliger

J. Stefan Institute
E. Kardelj University of Ljubljana
Ljubljana, Yugoslavia

I. INTRODUCTION

Liquid crystals are systems which flow like liquids while retaining the mechanical and optical anisotropy of crystals. On a microscopic level they are characterized by molecular orientational order accompanied by a partial or complete translational disorder of the molecular positions (1-3).

Thermotropic liquid crystals are formed upon heating many anisotropic organic compounds, while lyotropic liquid crystals are obtained by mixing amphiphilic compounds with water. Lyotropic liquid crystals are especially important in biology in view of their role in the structure of cell membranes.

Both thermotropic and lyotropic materials may exhibit more than one liquid crystalline phase. Smectic phases, whose specific property is the arrangement of the molecules into parallel layers, have been most intensively investigated during the last few years. Studies by means of miscibility relations (4-6), X-ray diffraction (7-15), nuclear magnetic resonance (16-21), nuclear quadrupole resonance,

and neutron scattering (22-27) have been very successful in the determination of the smectic structures and molecular dynamics.

The aim of this article is to review the contribution of ^{14}N nuclear quadrupole resonance (NQR) to the determination of orientational ordering in smectic liquid crystals. We shall discuss the orientational ordering in the smectic phases of achiral terephtal-bis-butyl-aniline (TBBA) and chiral terephtal-bis-amino-methyl-butyl-cinnamate (TBACA). The results will be compared with those obtained in the untilted smectic B phase of isobutyl-4-(4'-phenylbenzylidene-amino) cinnamate (IBPBAC). A perovskite-type layer structure compound $(C_{10}H_{21}NH_3)_2CdCl_4$, the hydrocarbon part of which represents a smectic bilayer embedded in a crystalline matrix, has also been investigated to explain the occurrence of two structural phase transitions similar to those in biological membranes.

In this review we describe first the structure of different smectic phases. To emphasize the importance of orientational molecular ordering for the understanding of liquid crystals, we also sketch the microscopic theories and describe the phenomenon of ferroelectricity in liquid crystals. Section III is devoted to the level crossing NQR double resonance method, which enables one to measure the ^{14}N spectra in liquid crystals. Section IV describes how to extract information on molecular ordering from the experimental NQR data. Finally, the ^{14}N NQR results, their analysis and discussion are presented in Section V.

II. SMECTIC LIQUID CRYSTALS

A. Structure of Smectic Phases

The term "smectic" includes a wide variety of liquid crystalline phases with the common feature that the centers of mass of the molecules are arranged in parallel equidistant planes. It is usually used for thermotropic liquid crystals. However, the lyotropic lamellar phase can also be described as "smectic" in view of its layered structure.

The most important aspects in the consideration of the structures of different smectic phases are:

i) the molecular translational order or disorder within the smectic layers,

ii) the possible occurrence of a tilt of the long molecular axes with respect to the normal of the smectic planes,

iii) the orientational ordering of the "short" molecular axes, and

iv) the stacking of the smectic layers one upon another.

We shall use the nomenclature of Helfrich (28) for the different smectic phases. According to the translational ordering of molecular positions within the layer, the smectic phases can be divided into:

1. disordered phases (Sm A and Sm C) and

2. ordered phases (Sm B, Sm H, Sm E, Sm G).

Beside these, there are several less investigated smectic structures which we shall not include here.

1. Disordered Smectic Phases

The smectic A phase. There is no long range translational order of the molecular positions within each layer. Sm A systems thus resemble a two-dimensional fluid. The preferred direction of the long axes of molecules, N, is perpendicular to the smectic layers (Figure 1). The layer thickness is close to the full length of the constituent molecules. The Sm A phase is optically uniaxial with the optical axis being normal to the plane of the layers.

The smectic C phase, which resembles the Sm A phase by the two-dimensional fluid character of the smectic layers, is optically biaxial. This is a

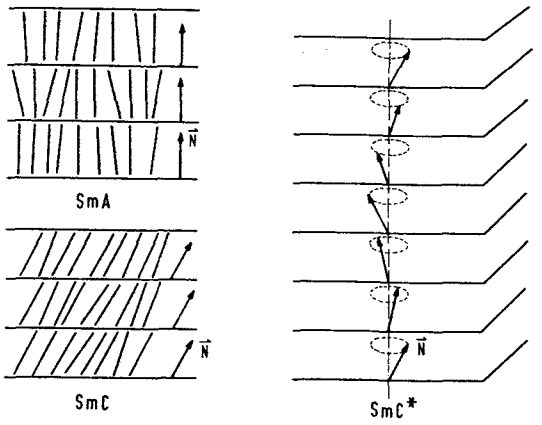

Figure 1. Schematic presentation of the Sm A, spatially homogeneous Sm C and spatially inhomogeneous, twisted Sm C* phase. The unit vector $\vec{N}$ points in the local preferred direction of the long molecular axes. The pitch of the helix in the Sm C* phase is much larger than the layer thickness (10^3 is a typical factor for their ratio).

consequence of the spontaneous collective tilt of the long molecular axes away from the layer normal. In achiral smectic C phases the tilt direction is constant in space. On the other hand, in chiral Sm C systems (Sm C*), where the molecules have a noncentrosymmetric atomic group, the direction of the tilt precesses around the layer normal on going from one layer to another and an incommensurate helicoidal Sm C* configuration is obtained (Figure 1). The molecular chirality induces thus a chirality in the structure of the Sm C* phase. The chiral Sm C* phase will be further discussed in connection with the phenomenon of ferroelectricity in liquid crystals.

2. Ordered Smectic Phases

In the translationally ordered smectic phases the molecular positions within a layer form a two-dimensional

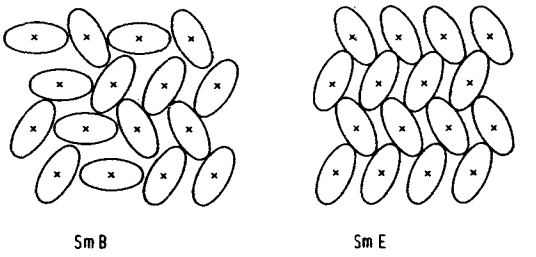

Figure 2. Schematic presentation of the molecular arrangement within a smectic plane in the hexagonally ordered Sm B (and Sm H) phases and in the "herringbone packed" Sm E (and Sm G) phases. Ellipses represent the molecular cross-section perpendicular to the long molecular axis.

lattice. In the orthogonal smectic B phase and the tilted smectic H phase, the two dimensional lattice is hexagonal or approximately hexagonal. Levelut et al. (12) have suggested on the basis of X-ray scattering that the molecules probably rotate by $\pi/3$ orientational jumps about their long axes and that the phenyl rings arrange themselves locally in a herring-bone type packing. The lattice parameter (5.18 Å) in TBBA is appreciably smaller than the size of the phenyl ring (~ 6.4 Å). They argue that the local orientational order is of higher symmetry than the average one (Figure 2).

By analogy with the twisted disordered Sm C* phase, an ordered Sm H* phase [called Sm III by the authors (29)] has been discovered in which the helicoidal arrangement of the tilt takes place. The chiral Sm H* phase has a similar hexagonal structure within the layer as the achiral Sm H phase except that the plane determined by the layer normal and the direction of the molecular tilt lies parallel to one edge of the hexagonal two-dimensional lattice in the chiral Sm H*

phase and perpendicular to one edge in the achiral phase.

The proposed two-dimensional lattice for the orthogonal smectic E phase and for the tilted smectic G phase is a herringbone arrangement of long range. The molecules should be able to rotate for an angle $\pi/2$ about their long axes (Figure 2).

The sequence of the various smectic phases with increasing temperature is such that the least ordered phases occur at the highest temperatures (Table 1).

B. Microscopic Theories of Smectic Phases

Concurrent with experimental investigations of smectic structures, theories have been developed to describe the properties of different smectic phases and the transitions among them. The main contribution of NQR to the physics of liquid crystals has been the determination of the local orientational ordering of the short molecular axes, which is of basic importance for the microscopic theories of the smectic phases.

McMillan and Meyer (30-33) have developed the microscopic theory of the Sm A phase, the Sm C phase, of the ordered Sm B and Sm H phases and of the Sm E phase. Other authors have studied the Sm A → Sm C transition and the corresponding structure of the smectic C phase. The models of the Sm C phase have been developed by McMillan (31), Wulf (34-35), Priest (36), Cabib and Benguigui (37), and Van der Meer and Vertogen (38). In those theories different forces among molecules are stated to be responsible for the onset of the Sm C phase. According to some of them the freezing out of molecular rotation around the long axis is required for the onset of the tilted phases, while others leave the rotation free or nearly free throughout the Sm C phase as shown in Table 2. It is exactly this problem that has been succesfully solved by using ^{14}N NQR.

In the following a short description will be given of two microscopic theories of smectic phases: that of McMillan and Meyer (30,32), which includes most of the known smectic phases, and that of Van der Meer and Vertogen (38), which is the newest and seems to solve many long-standing problems.

1. McMillan-Meyer Theory

McMillan first developed the microscopic theory of the Sm A phase (30) by assuming a special interaction between anisotropic molecules which is proportional to:

$$\exp-[(r_{12}/r_0)^2][(3/2)\cos^2\theta_{12} - 1/2].$$

Here r_{12} is the distance between centers of mass of two molecules, θ_{12} the angle between the directions of their long axes and r_0 is roughly a molecular length. With this potential he showed that it is energetically favorable for the oriented molecules to arrange themselves below a definite temperature into smectic layers instead of being randomly distributed in space as in the nematic phase. The orientational order parameter S (often called the "nematic order parameter") is defined as

$$S = (1/2)\langle 3\cos^2\theta - 1\rangle \qquad (1)$$

with θ denoting the angle between the long axis of one molecule and the local preferred direction. S increases nearly continuously from the nematic to the smectic A phase. On the other hand, the "Sm A order parameter" σ, representing the amplitude of a density wave in the direction perpendicular to the long molecular axes, assumes values different from zero only in the smectic phases.

With the aim of developing further a comprehensive theory, which would include both disordered smectic phases (Sm A and Sm C) and the two ordered phases with hexagonal structure, McMillan and Meyer (32) studied the system in which both arrangement of the molecules into smectic planes and perfect orientational order are already well established. The intermolecular potential is then taken to be due to electric dipole-dipole interactions due to permanent dipole moments and soft-core repulsion between the molecules. A molecule is supposed to be a long rod

Table 1. The Scheme of Established Smectic Liquid Crystalline Phases and their Structures (28)

	Smectic liquid crystals		
	Ordered		Disordered
	Herringbone	Hexagonal (or nearly hexagonal)	
orthogonal	E	B	A
tilted	G	H	C
tilted and twisted		H*(III)	C*
		---------->	
		rising temperature	

Table 2. Models of the Sm C Phase

Authors	Interactions between molecules	Orientational ordering
McMillan	Dipole-dipole forces (between permanent electric dipoles on neighboring molecules)	Rotation around the long molecular axis is frozen out
Wulf	Steric forces	Rotation is frozen out
Priest	General coupling	Free rotation or nearly free
Cabib, Benguigui	Dipole-dipole forces (only between components parallel to the long molecular axes)	Free rotation
Van der Meer, Vertogen	Forces between permanent and induced dipoles	Free rotation

of diameter D with oppositely directed permanent dipoles on opposite sites of the molecular centre (Figure 3). According to this model the interaction U_{12} between two molecules in the plane can be written as:

$$U_{12} = \left[\frac{\vec{\mu}_1 \cdot \vec{\mu}_2}{r_{12}^3} - \frac{3(\vec{\mu}_1 \cdot \vec{r}_{12})(\vec{\mu}_2 \cdot \vec{r}_{12})}{r_{12}^5} \right] \times S(r_{12}) + T(r_{12}) . \quad (2)$$

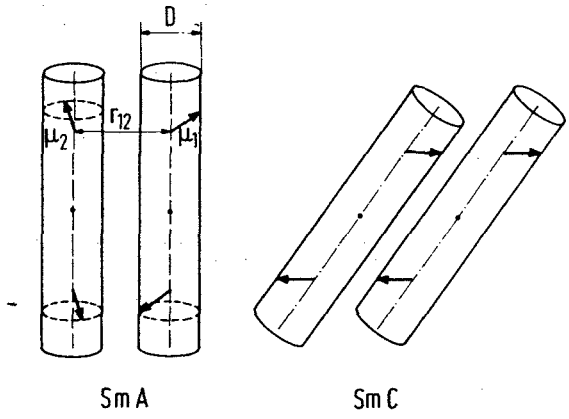

Figure 3. McMillan's model of the orthogonal Sm A and of the tilted Sm C phase. The orientational ordering of permanent electric dipoles is responsible for the onset of the tilt.

The first term in the above potential represents dipole-dipole interaction between two dipoles at a distance $\vec{r}_{12}$ apart. $S(r_{12})$ is the two-particle correlation function which is zero for $r_{12} < D$ and different from zero for $r_{12} > D$. The second term, $T(r_{12})$, in equation 2 is a soft-core repulsive potential whose magnitude is V_0 for $r_{12} < D$ and zero outside this region. The interlayer interactions as well as the interaction between dipoles on different levels have been neglected as the spacing between the two dipoles on one molecule is larger than the intermolecular spacing.

The authors have solved the above model within the mean field approximation. The self-consistency requirement gives the following equations for the order parameters:

$$\alpha = (1/3)\langle \cos\vec{K}_1 \cdot \vec{x} + \cos\vec{K}_2 \cdot \vec{x} + \cos\vec{K}_3 \cdot \vec{x} \rangle \quad (3a)$$

$$\beta = \langle \cos\psi \rangle \quad (3b)$$

$$\gamma = (1/3)\langle \cos\psi (\cos\vec{K}_1 \cdot \vec{x} + \cos\vec{K}_2 \cdot \vec{x} + \cos\vec{K}_3 \cdot \vec{x}) \rangle . \quad (3c)$$

Here $\vec{x}$ is the coordinate in the smectic plane on the level of molecular dipoles, $\vec{K}_1$, $\vec{K}_2$, and $\vec{K}_3$ are the reciprocal vectors of the hexagonal lattice and ψ is the azimuthal angle determining the instantaneous molecular orientation during its rotation about the long axis.

The orientational order parameter is β. When β is finite, the rotation around the long molecular axis is biased and the dipoles are aligned parallel to an axis lying in the smectic plane (Figure 3). Though there is no net dipole moment, the liquid crystal is biaxial and tilted. With $\beta = 0$, the liquid crystal is uniaxial, untilted, and there is no orientational order.

The translational order parameter is α. When α is finite, the molecules lie on a two-dimensional hexagonal lattice in each smectic plane. When $\alpha = 0$, the molecules move as a two-dimensional liquid.

The order parameter γ describes the coupling between the translational and orientational order and is finite only when both α and β are finite.

Depending on the values of the parameters involved in the calculation, four characteristic sets of solutions for the order parameters can be obtained:

i) $\alpha = \beta = \gamma = 0$, no translational and orientational order in the smectic plane (Sm A)

ii) $\alpha \neq 0$, $\beta = \gamma = 0$, translational order in smectic Sm plane, no

orientational order (Sm B)

iii) $\alpha = \gamma = 0$, $\beta \neq 0$, no translational order, orientational order of dipoles in plane (Sm C)

iv) $\alpha \neq 0$, $\beta \neq 0$, $\gamma \neq 0$, translational and orientational order in plane (Sm H).

The temperature dependence of order parameters and the phase diagrams have been determined for some definite values of the soft-core repulsive potential V_0 and parameter B which depends on the two-particle positional correlation function. In Figure 4 a typical

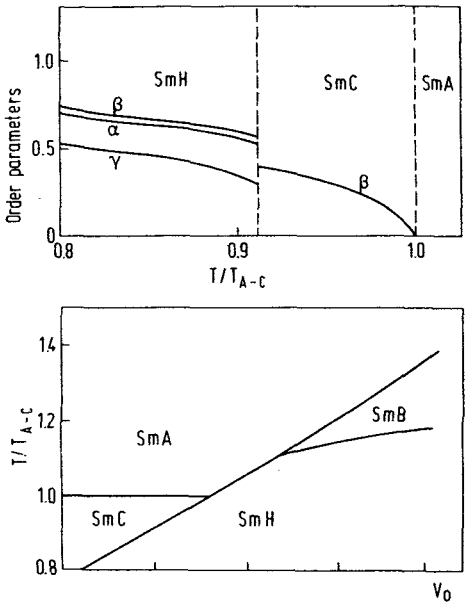

Figure 4. Temperature dependence of order parameters α, β and γ predicted by the Meyer-McMillan theory and a phase diagram showing the onset of different smectic phases with increasing value of the intermolecular soft-core repulsive potential V_0 (32).

temperature dependence of the order parameters is presented for the phase sequence Sm A $\leftrightarrow$ Sm C $\leftrightarrow$ Sm H. Clearly the calculated Sm A $\leftrightarrow$ Sm C transition is second order while the Sm C $\leftrightarrow$ Sm H transition is first order. It is also found that the Sm B $\leftrightarrow$ Sm H transition is of second order while others are of first order. The predicted orientational order parameter β in the Sm H phase is between 0.3 and 0.5. In the lower part of Figure 4 a phase diagram is shown for B = 23.1. The Sm C phase appears at low values of V_0. According to this theory the Sm C phase may be expected in compounds where the molecular structure is dominated by two outboard oppositely directed dipoles. The Sm B phase occurs at high V_0, that is in the cases where the molecular structure is dominated by the repulsive soft-core potential.

Meyer extended the above theory to obtain the onset of the Sm E phase as well (33). He included in addition to dipole-dipole and soft-core intermolecular forces a phenyl-phenyl interaction of the Van der Waals type.

2. Van der Meer-Vertogen Theory

Van der Meer and Vertogen (38) developed a microscopic theory which is based on induced dipole forces between molecules and accounts for the nematic, Sm A, and Sm C phase. Their theory considers a model in which the molecule is a rod-like object with an isotropically polarizable unit at its center. Any atomic group within a given molecule with a permanent electric dipole will induce a dipole in the center of a neighboring molecule. The induction forces of this type are responsible for the onset of the tilt in the Sm C phase. Even free rotation of the molecule about its long axis does not destroy this concept because induction forces, in contrast to McMillan's dipole-dipole forces, are not averaged out by this rotation.

The above model has been solved within the mean field approximation to yield the values of the nematic order parameter S, "Sm A order parameter" σ and the tilt angle θ_0. Four different sets of solutions refer to the following phases:

$S = 0$, $\sigma = 0$, $\theta_0 = 0$ - isotropic phase

$S \neq 0$, $\sigma = 0$, $\theta_0 = 0$ - nematic phase

$S \neq 0$, $\sigma \neq 0$, $\theta_0 = 0$ - smectic A phase

$S \neq 0$, $\sigma \neq 0$, $\theta_0 \neq 0$ - smectic C phase.

C. Ferroelectric Liquid Crystals

Ferroelectricity in liquid crystals can occur in two different situations:

In uniaxial liquid crystals, such as the nematic and smectic A phase, the spontaneous polarization can be non-zero only if "head to tail" ordering takes place. In such a case the spontaneous polarization would be parallel to the average direction of the long molecular axes. No direct experimental proof of ferroelectricity in uniaxial liquid crystals has been obtained until now.

In biaxial liquid crystals, such as the chiral smectic C* and smectic H* phases, there may be a non zero component of the molecular dipole moment normal to the direction of the long molecular axis and parallel to the smectic layer. This follows from symmetry considerations (39).

In such systems ferroelectricity and in-plane spontaneous polarization have indeed been observed by Meyer et al. (39). The system under study was p-decyloxybenzylidene-p'-amino-2-methyl-butylcinnamate (DOBAMBC)

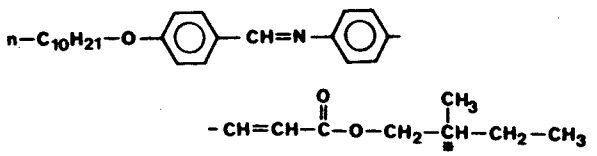

The methyl-butyl group is responsible for the chirality of the molecule. In its vicinity is the polar ester group. The sequence of the phase transitions in DOBAMBC is the following (T in °C):

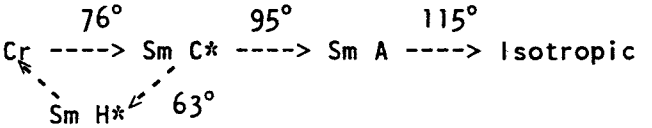

Ferroelectric properties have been observed in the Sm C* and the Sm H* phase. The direction of the spontaneous polarization, which is perpendicular to the direction of the long molecular axis, precesses from one layer to the next around the normal to the layers in the same way as the molecular tilt. Each layer is ferroelectrically ordered but the whole sample represents a helicoidal antiferroelectric with zero net polarization. Since the distance between the smectic layers is an irrational fraction of the pitch of the helix, ferroelectric liquid crystals represent structurally incommensurate systems. The effective dipole moment per molecule is equal to ~ 0.05 Debye in the Sm C* phase. This value is 10-100 times smaller than in solid ferroelectrics and represents only a few percent of the calculated value for the permanent electric dipole per molecule (~ 1 Debye). This discrepancy can be explained by the partial averaging out of the dipoles due to the partially biased rotation of molecules about their long axes.

The interactions among effective molecular dipoles in liquid crystals are too weak to produce the ferroelectric ordering themselves. The transition from the Sm A to the Sm C* phase is driven by intermolecular forces producing the onset of the tilt. The spontaneous polarization which appears in the Sm C* phase is only a secondary effect induced by the Sm C* liquid crystalline ordering. Ferroelectric liquid crystals are thus improper ferroelectrics.

It is easily shown (40) that the polarization is proportional to the tilt angle θ_0, and decreases continuously to zero at the transition temperature from the Sm C* to the Sm A phase, T_c. Above T_c the free energy density g of a non-equilibrium state can be expanded in powers of the in-plane polarization $\vec{P}_\perp$ and tilt angle $\vec{\theta} = \vec{\nu} \times \vec{N}$, which is considered as the Sm. C order parameter. Here $\vec{\nu}$ is

the normal to the smectic planes and $\hat{N}$ the unit vector specifying the direction of the long molecular axis.

In the spatially homogeneous case we find

$$g = g_A + (1/2)A(T)\left|\hat{\theta}\right|^2 + (1/4)B\left|\hat{\theta}\right|^4 + (1/2)\kappa(T)\left|\hat{P}_\perp\right|^2 - \xi\hat{\Theta}\cdot\hat{P}_\perp . \quad (4)$$

The coefficient $A(T) = a(T - T_0)$ accounts for the short range driving force of the pure Sm A → Sm C* transition whereas $\kappa(T) = a'(T - T_0')$ accounts for the driving force of the pure ferroelectric transition. All other coefficients are assumed to be temperature independent. The linear coupling between the tilt and the polarization is allowed by symmetry.

The problem can be simplified by choosing a special coordinate system, where the two-fold rotation axis, and hence $\hat{P}_\perp$, is perpendicular to the plane determined by the layer normal $\hat{\nu}$ and $\hat{N}$.

The equilibrium values θ_0 and P_0 of the tilt and polarization are obtained from the requirements:

$$(\partial g/\partial\theta)_{\theta_0,P_0} = 0 ,$$

$$(\partial g/\partial P_\perp)_{\theta_0,P_0} = 0 . \quad (5)$$

It can be seen immediately that the spontaneous polarization is proportional to the tilt angle:

$$P_0 = (\xi/\kappa)\theta_0 . \quad (6)$$

To take into account the spatial inhomogeneity of the Sm C* phase theories have been developed (41) which include the inhomogeneous Lifshitz term in addition to the terms in equation 4. Interesting effects such as the existence of the Lifshitz tricritical point in the E-T phase diagram, which have been predicted (42), are beyond the scope of this paper.

III. PROTON-NITROGEN LEVEL CROSSING DOUBLE RESONANCE

The signal of the nitrogen nuclei in liquid crystals is too weak to be detected by standard NQR techniques. Therefore a nuclear double resonance technique, introduced by Hartmann and Hahn (43) and later Lurie and Slichter (44), is employed which uses the "strong" NMR signal of the spins I to detect the "weak" NMR or NQR signal of the spins S. The sensitivity of this method may be several orders of magnitude greater than the sensitivity of classical magnetic or quadrupole resonance techniques. The spectra of the spins S can be measured with practically the same sensitivity as the spectra of the I spins.

The double resonance techniques are based on the existence of nuclear dipole-dipole coupling between the two spin systems, which takes place when the energy levels of the I and S spins are equally spaced. The "resonant" coupling can be established either in the rotating or dipolar frame or in the laboratory frame. In the latter case at least one of the spin species must exhibit a non-zero quadrupole splitting in addition to the Zeeman splitting for resonant energy transfer to occur.

Measurements of ^{14}N NQR spectra in smectic liquid crystals have been performed with the help of a simple proton-nitrogen double resonance technique involving level crossing in the laboratory frame. Since an excellent review of the double resonance method has been published recently in this journal (45), we shall only briefly sketch the basic principles of our experiment.

^{14}N is a nucleus with spin S = 1. The interaction of its electric quadrupole moment with the electric field gradient $V_{ij} = (\partial^2 V)/(\partial x_i \partial x_j)$ at the nuclear site gives rise to three pure quadrupole energy levels in the absence of external magnetic field. Their energies are (46):

$$E_+ = (1/4)e^2qQ(1 + \eta)$$

$$E_- = (1/4)e^2qQ(1 - \eta) \quad (7)$$

$$E_0 = -(1/2)e^2qQ.$$

Here eQ denotes the scalar quadrupole moment of the ^{14}N nucleus and eq the largest eigenvalue V_{ZZ} of the local

electric field gradient (EFG) tensor. Their product e^2qQ/h is the ^{14}N quadrupole coupling constant. The asymmetry parameter η reflects the deviation of the EFG tensor at the nuclear site from cylindrical symmetry. It is defined as $|(V_{XX} - V_{YY})|/V_{ZZ}$, where V_{XX} and V_{YY} are the smaller two eigenvalues of the EFG tensor. All transitions between the three quadrupole energy levels are allowed. The corresponding resonant frequencies are:

$$\nu_+ = (3/4)(e^2qQ/h)(1 + \eta/3)$$

$$\nu_- = (3/4)(e^2qQ/h)(1 - \eta/3) \qquad (8)$$

$$\nu_0 = \nu_+ - \nu_- = (1/2)\eta e^2qQ/h \ .$$

If the sample is put in a magnetic field of strength B, the Zeeman interaction of the ^{14}N magnetic dipole moments with the magnetic field has to be taken into account as well. The magnetic coupling can be treated as a small perturbation up to fields of ~100 Gauss. The magnetic interaction causes a slight increase of the E_+ energy level and a slight decrease of the E_- and E_0 energy levels, as presented in Figure 5. It can be shown (47) that for a powder sample the transition frequencies ν_+^1, ν_-^1, and ν_0^1 between the Zeeman perturbed quadrupole energy levels of nitrogen are:

$$\nu_+^1 = \nu_+ + (1/3)\nu_{L,N}^2(1/\nu_0+2/\nu_++1/\nu_-)$$

$$\nu_-^1 = \nu_- + (1/3)\nu_{L,N}^2(-1/\nu_0+2/\nu_-+1/\nu_+)$$

$$\nu_0^1 = \nu_0 + (1/3)\nu_{L,N}^2(2/\nu_0+1/\nu_+-1/\nu_-) . \qquad (9)$$

Here $\nu_{L,N}$ is the pure Zeeman transition frequency given by $\nu_{L,N} = \gamma_N B/2\pi$. The values of $\nu_{L,N}$ are relatively small in view of the low nitrogen gyromagnetic ratio γ_N, thus justifying the perturbation treatment used in the evaluation of equations 9.

In contrast to the ^{14}N case the protonic quadrupole moment is zero. As the proton gyromagnetic ratio is 13.4 times larger than the nitrogen one, the protonic energy levels cross the levels of the ^{14}N nuclei at a sufficiently high value of the magnetic field. At

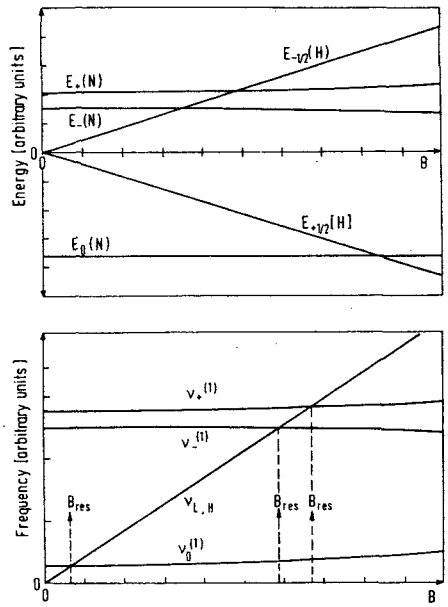

Figure 5. Energy levels and the corresponding transition frequencies of ^{14}N nuclei and protons in low magnetic field. B_{res} denotes the values of the magnetic field at which the coupling between nitrogen nuclei and protons takes place.

three definite values of the magnetic field B the nitrogen and proton ($\nu_{L,H}$) transition frequencies become equal (Figure 5), and cross relaxation between the proton and nitrogen system takes place, thus enabling one to measure the quadrupole resonance frequencies of ^{14}N via the proton signal.

The experiment is performed as follows. The sample is placed first in a high magnetic field B_0 where the protons are polarized, creating a net magnetization M_{B_0}. Then the sample is moved with a pneumatic post to a low magnetic field B, where the protons are allowed to relax for a fixed time $t = \tau$. The sample is subsequently moved back to B_0 and the remaining proton magnetization M is measured with a 90° rf pulse. The magnetization is

given by (47)

$$M(t) = M_{B_0}(1 - B/B_0)\exp(-t/T_{1B}) + M_{B_0}(B/B_0) \quad , \qquad (10)$$

where T_{1B} is the proton spin-lattice relaxation time in the field B. The same procedure is repeated for different values of the low magnetic field B until a complete dependence

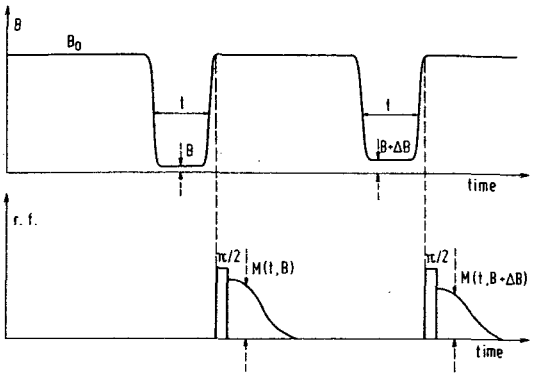

Figure 6. Magnetic field and r.f. pulse sequences used in the proton-nitrogen level crossing double resonance.

$M(t) = M(t,B)$ is obtained (Figure 6). The Zeeman perturbed ^{14}N NQR frequencies ν^1 are determined by observing the dips in the magnetic field dependence of the proton magnetization. An example is shown in Figure 7.

Because of the short proton-nitrogen cross relaxation times (usually smaller than 1 msec), the depth of the dip is determined by the actual change in the proton spin-lattice relaxation time T_{1B} at the cross-over. The change strongly depends on the difference between the proton T^0_{1B} (the spin-lattice relaxation time due to all other processes but cross relaxation to the ^{14}N nuclei) and the ^{14}N quadrupole spin-lattice relaxation time T_{1Q}. The depth of the dip and thus the

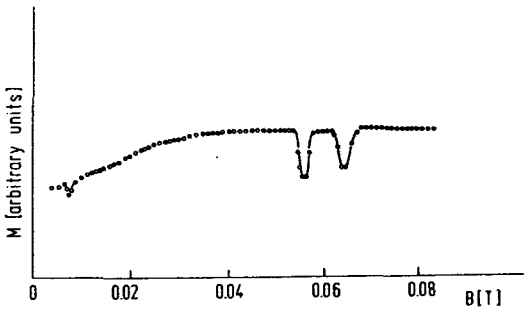

Figure 7. An example of proton-^{14}N cross-over relaxation spectra.

sensitivity of the method is highest for $T^0_{1B} >> T_{1Q}$. The width of the dip is determined by the broadening of the proton Larmor frequency $\nu_{L,H}$ due to the dipole interaction with neighboring nuclei and by Zeeman broadening of the ^{14}N NQR powder spectrum.

The advantages of this direct level crossing proton-nitrogen detection compared to other double resonance techniques are its simplicity, the fact that powdered samples can be used instead of well aligned single crystalline samples, and the fact that the spin quenching effect is avoided. It should be noted, however, that the method is applicable only for samples in which the proton T_1 is long enough ($\gtrsim$ 200 msec) to allow for transfer of the sample from the high to the low magnetic field in a time short compared to T_1.

IV. THE RELATION BETWEEN THE NQR DATA AND THE ORIENTATIONAL ORDER PARAMETERS

If the correlation frequency of the molecular motion is much larger than the ^{14}N NQR frequencies, which is usually the case in liquid crystals, the observed value of the EFG tensor represents a time average over the molecular motion. This is smaller than the rigid

lattice value observed in solids. The central problem concerns the nature of the molecular motion producing a given time average.

Some qualitative facts on the molecular motion can be immediately obtained from the measured values of e^2qQ/h and η. A comparison between the observed and rigid lattice values of e^2qQ/h characterizes the degree of motional averaging and reflects the amplitudes of the molecular motion. The asymmetry parameter η is zero for unhindered rotation around the long molecular axis, while non-zero value indicates a deviation from cylindrical symmetry at the nucleus and thus an anisotropy in the molecular motion.

To quantitatively describe the molecular motion, the relations linking the values of e^2qQ/h and η to the order parameters should be properly deduced. These relations have been discussed (48-51).

In the rigid crystal the ^{14}N EFG tensor can be written (49) in the molecular frame x_o, y_o, z_o as

$$V_{ij} = \begin{pmatrix} V_{x_ox_o} & V_{x_oy_o} & V_{x_oz_o} \\ V_{x_oy_o} & V_{y_oy_o} & V_{y_oz_o} \\ V_{x_oz_o} & V_{y_oz_o} & V_{z_oz_o} \end{pmatrix} \quad . (11)$$

The molecular frame is normally chosen with the z_o axis parallel to the long axis of the molecule. The choice of the y_o direction depends on the particular molecular group under study. The x_o axis is perpendicular to y_o and z_o, so that x_o, y_o, z_o represent an orthogonal right handed system.

If the observed ^{14}N nucleus belongs to the nearly planar C-N=CH-C linkage group, as in the present case, it is convenient to choose y_o normal to this plane. It is known from work on other Schiff's bases that the largest principal axis of the ^{14}N EFG tensor lies then in the x_oz_o plane and makes an angle of about 60° with the z_o axis, while $V_{x_oy_o}$ and $V_{y_oz_o}$ should be small. The exact values of the V_{ij} tensor can be determined from a complete set of single-crystal rotation data.

If the five independent EFG tensor components in the molecular frame are known and a model for molecular motion is assumed, the components of the time averaged EFG tensor can be evaluated (49). The principal values of the time averaged tensor, obtained by diagonalization, provide the relations between the observed values of e^2qQ/h and η on one side and the order parameters on the other.

In the smectic phases the molecular rotation about the long axis is expected to govern the time averaging of the EFG tensor at ^{14}N sites. In some phases, especially in the disordered ones, the fluctuations in the direction of the long axis can be significant as well.

A. Averaging due to Rotation around the Long Axis

The molecule is assumed to perform a hindered rotation around the long molecular axis, i.e. it jumps between several equilibrium orientations. To take into account this motion the EFG tensor (equation 11) is transformed from the molecular x_o, y_o, z_o frame into a frame x, y, $z \| z_o$, where $z \| z_o$ is the axis of rotation and $\psi = \psi(t)$ is the angle between x and x_o. The EFG tensor is expressed in the x, y, z frame as:

$$\begin{aligned} V_{xx} &= -(1/2)V_{z_oz_o} + (1/2)(V_{x_ox_o} - V_{y_oy_o})\cos 2\psi - V_{x_oy_o}\sin 2\psi \\ V_{xy} &= (1/2)(V_{x_ox_o} - V_{y_oy_o})\sin 2\psi + V_{x_oy_o}\cos 2\psi \ , \\ V_{xz} &= V_{x_oz_o}\cos\psi - V_{y_oz_o}\sin\psi \ , \qquad (12) \\ V_{yy} &= -(1/2)V_{z_oz_o} - (1/2)(V_{x_ox_o} - V_{y_oy_o})\cos 2\psi + V_{x_oy_o}\sin 2\psi, \\ V_{yz} &= V_{x_oz_o}\sin\psi + V_{y_oz_o}\cos\psi, \\ V_{zz} &= V_{z_oz_o} \ . \end{aligned}$$

When equation 12 is averaged over the molecular motion, we have to replace

$\cos\psi$ by $\langle\cos\psi\rangle$ etc. The mean values $\langle\cos\psi\rangle$, $\langle\cos2\psi\rangle$, etc. play the role of order parameters which are characteristic for the given type of orientational ordering.

1. Uniaxial Rotation without Biasing

In the case when all equilibrium orientations by molecular rotation around the long axis are equivalent, the above order parameters equal zero:

$$\langle\cos\psi\rangle = \langle\cos2\psi\rangle = \langle\sin\psi\rangle = \langle\sin2\psi\rangle = 0.$$

The largest eigenvalue of averaged EFG tensor is $V_{ZZ} = \langle V_{zz}\rangle = V_{z_0z_0}$, yielding a temperature independent quadrupole coupling constant e^2qQ/h and a zero value of the asymmetry parameter $\eta = 0$.

2. Uniaxial Rotation with Polar Biasing

In the case of a polar partial rotational freeze-out the effective potential felt by each molecule has the form $V = -V'(\cos\psi)$. The resulting orientational ordering is polar with characteristic order parameters $\langle\cos\psi\rangle \neq 0$, $\langle\cos2\psi\rangle \neq 0$, and $\langle\sin\psi\rangle = 0$, $\langle\sin2\psi\rangle = 0$. The values of $\langle\cos\psi\rangle$ and $\langle\cos2\psi\rangle$ can be given in terms of modified Bessel functions as

$$\langle\cos\psi\rangle = I_1(a)/I_0(a), \quad a = V'/(kT) \tag{13}$$

$$\langle\cos2\psi\rangle = I_2(a)/I_0(a), \quad a = V'/(kT) .$$

If the orientational ordering is weak (i.e. if $V'\ll kT$) the Bessel functions may be expanded to obtain:

$$\langle\cos2\psi\rangle \simeq (1/2)\langle\cos\psi\rangle^2 \ll \langle\cos\psi\rangle. \tag{14}$$

The only relevant order parameter for weak polar ordering is thus $\langle\cos\psi\rangle$, while $\langle\cos2\psi\rangle$ can be neglected. The resulting values for e^2qQ/h and η are:

$$e^2qQ/h = (eQV_{z_0z_0}/h)[1 + (2/3)(V_{x_0z_0}^2 + V_{y_0z_0}^2)/V_{z_0z_0}^2 \times \langle\cos\psi\rangle^2]$$

$$= eQV_{z_0z_0}(1 + \eta) ,$$

$$\eta = (2/3)[(V_{x_0z_0}^2 + V_{y_0z_0}^2)/V_{z_0z_0}^2]\langle\cos\psi\rangle^2 .$$

We thus see that for biased rotation η is different from zero. The temperature dependence of η reflects the temperature change of the square of the polar order parameter $\langle\cos\psi\rangle$.

3. Uniaxial Rotation with Bipolar Biasing

Bipolar orientational order takes place in a potential of the form $V = -V'(\cos2\psi)$. In this case $\langle\cos2\psi\rangle \neq 0$, $\langle\cos\psi\rangle = 0$, and $\langle\sin\psi\rangle = 0$, $\langle\sin2\psi\rangle = 0$.

If the bipolar orientational ordering is weak ($\langle\cos2\psi\rangle \ll 1$) the largest principal axis of the ^{14}N EFG tensor still points along the axis of rotation (z_0). The quadrupole coupling constant and the asymmetry parameter are:

$$eQV_{zz}/h = eQV_{z_0z_0}/h ,$$

$$\eta = r\langle\cos2\psi\rangle , \tag{16}$$

where

$$r = 2[V_{x_0y_0}^2 + (1/4)\times(V_{x_0x_0} - V_{y_0y_0})^2]^{1/2}/V_{z_0z_0} .$$

We see that η depends linearly on $\langle\cos2\psi\rangle$ and hence is temperature dependent, whereas e^2qQ/h is constant.

For large values of $\langle\cos2\psi\rangle$ the largest principal axis of the ^{14}N EFG tensor no longer points along the axis of rotation. For the nitrogen in the C-CH=N-C group it lies in the x_0z_0 plane. For $(r\langle\cos2\psi\rangle) > 1$ we find:

$$eQV_{zz}/h = -(1/2h)eQV_{z_0z_0}(1 + r\langle\cos2\psi\rangle)$$

and (17)

$$\eta = \left|\frac{r\langle\cos2\psi\rangle - 3}{r\langle\cos2\psi\rangle + 1}\right| ,$$

so that both e^2qQ/h and η depend on

$\langle\cos 2\psi\rangle$ and are temperature dependent.

B. Additional Averaging due to Fluctuations in the Direction of the Long Axis

The fluctuations in the direction of the long molecular axis, in addition to rotations around this axis, are taken into account by performing still another transformation of the EFG tensor given by equation 12 to a fixed x', y', z' frame, where z' is normal to the smectic planes, x' is the direction of the average projection of the long molecular axis on the smectic plane, and y' is perpendicular to x' and z'. The angles $\Theta = \Theta(t)$ and $\phi = \phi(t)$ are the polar and azimuthal angles, respectively, determining the direction of the long molecular axis in the x', y', z' frame. $\Theta(t)$ can be approximately written as $\Theta(t) = \Theta_0 + \delta\Theta(t)$, where Θ_0 denotes the well known tilt angle (Figure 8).

After this second transformation has been performed the time averaged values of the ^{14}N EFG tensor are (49):

$$\langle V_{x'x'}\rangle = \langle (V_{zz} - V_{xx})\sin^2\Theta\cos^2\phi\rangle + \langle V_{xx}\cos^2\phi\rangle + \langle V_{yy}\sin^2\phi\rangle + \langle V_{xz}\sin 2\Theta\cos^2\phi\rangle ,$$

$$\langle V_{x'y'}\rangle = \langle V_{yz}\sin\Theta\cos 2\phi\rangle + \langle V_{xy}\cos\Theta\cos 2\phi\rangle ,$$

$$\langle V_{x'z'}\rangle = \langle (V_{zz} - V_{xx})\sin\Theta\cos\Theta\cos\phi\rangle + \langle V_{xz}\cos 2\Theta\cos\phi\rangle ,$$

$$\langle V_{y'y'}\rangle = \langle (V_{zz} - V_{xx})\sin^2\Theta\sin^2\phi\rangle + \langle V_{xx}\sin^2\phi\rangle + \langle V_{yy}\cos^2\phi\rangle + \langle V_{xz}\sin 2\Theta\sin^2\phi\rangle,$$

$$\langle V_{y'z'}\rangle = -\langle V_{xy}\sin\Theta\cos\phi\rangle + \langle V_{yz}\cos\Theta\cos\phi\rangle ,$$

$$\langle V_{z'z'}\rangle = -\langle (V_{zz} - V_{xx})\sin^2\Theta\rangle + \langle V_{zz}\rangle - \langle V_{xz}\sin 2\Theta\rangle . \quad (18)$$

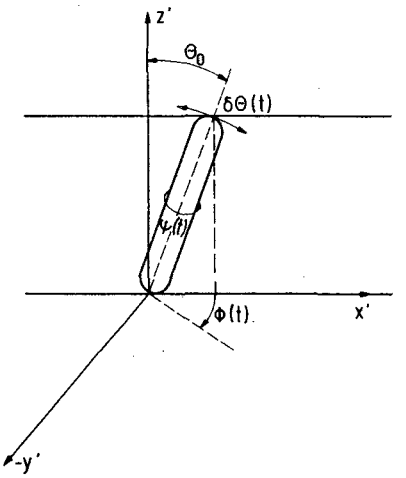

Figure 8. Schematic presentation of a tilted molecule within a smectic layer. Θ_0 is the average tilt angle, $\delta\Theta(t)$ denotes the fluctuations in the orientation of the long molecular axis in the polar direction, and $\phi(t)$ the fluctuations in the azimuthal direction. $\psi(t)$ denotes the orientation of the short molecular axes during the molecular rotation around its long axis.

In this set of equations a large number of different order parameters appear. Those that are functions of ψ describe the order around the long molecular axis, while those that are functions of Θ and ϕ describe the ordering of the long molecular axis itself. The algebraic relations between e^2qQ/h and η and the values of the EFG tensor in the x', y', z' frame are rather complicated. If, however, the fluctuations in Θ, ϕ and ψ are assumed to be independent and are small enough to allow the expansion of the sine and cosine of Θ and ϕ in a power series, relatively simple expressions for e^2qQ/h and η can be obtained. For the case of weak bipolar ordering we find:

$$e^2qQ \simeq eQV_{z_0z_0}[1 - (3/2)\langle\delta\Theta^2\rangle - (3/2)\Theta_0^2(1 - \langle\cos\phi\rangle^2)]$$

and

$$\eta \simeq (3/2)\Theta_0^2(\langle\cos\phi\rangle^2 - \langle\cos 2\phi\rangle) - (3/2)\langle\delta\Theta^2\rangle\langle\cos 2\phi\rangle - [(V_{x_0x_0} - V_{y_0y_0})/V_{z_0z_0}]\times \langle\cos 2\phi\rangle\langle\cos 2\psi\rangle \quad (19)$$

Equation 19 shows the combined effects of both bipolar biasing and anisotropic fluctuations in the direction of the long axis on the values of e^2qQ/h and η. In the first approximation e^2qQ/h does not depend on the orientational ordering $\langle\cos 2\psi\rangle$ but is mainly determined by the mean square fluctuations in the polar angle $\langle\delta\Theta^2\rangle$. In contrast to e^2qQ/h, η does depend on the orientational order parameter $\langle\cos 2\psi\rangle$ through the last term in equation 19. This term is however rather small in the Sm C phase for which the above model is appropriate. The prevailing term which produces the characteristic maximum in the temperature dependence of η is $(3/2)\langle\delta\Theta^2\rangle\langle\cos 2\phi\rangle$. In the low temperature part of the smectic C phase, $\langle\cos 2\phi\rangle \simeq 1$ and η increases with increasing temperature due to the increase in $\langle\delta\Theta^2\rangle$. At higher temperatures, η decreases as $\langle\cos 2\phi\rangle \to 0$, so that there has to be a maximum in between.

Anisotropic fluctuations in the direction of the long molecular axis by themselves result in a nonzero value of η though there is no biasing of the rotation around the long axis. In this case we find

$$e^2qQ = eQV_{z_0z_0}[1 + (3/2)(\langle\sin\Theta\cos\Theta\cos\phi\rangle^2 - \langle\cos^2\Theta\rangle\langle\sin^2\Theta\cos^2\phi\rangle - \langle\sin^2\Theta\sin^2\phi\rangle)] \quad (20)$$

and

$$\eta = (3/2)(\langle\sin\Theta\cos\Theta\cos\phi\rangle^2 - \langle\cos^2\Theta\rangle\langle\sin^2\Theta\cos^2\phi\rangle + \langle\sin^2\Theta\sin^2\phi\rangle) .$$

The two different mechanisms leading to a finite value of η, orientational ordering and anisotropic fluctuations in the long molecular axis, can be easily discriminated in view of the different temperature dependences they predict for η and e^2qQ/h.

A different approach to the problem of relations among e^2qQ/h and η and order parameters has been developed by Allender and Doane (51). They obtained the expression for η without assuming a special model for molecular motion and evaluated η for the general case and for the limiting cases of uniform rotation or biased rotation without fluctuations.

It should be stressed that it is not possible to determine by NQR the values of all possible different order parameters as there are at each temperature only two experimental parameters available (e^2qQ/h and η). The problem is often simplified by additional information on the symmetry of the molecular motion deduced from X-ray or other experiments.

V. EXPERIMENTAL RESULTS AND DISCUSSION

A. Achiral Smectic TBBA

Terephtal-bis-butylaniline (TBBA) has been the most extensively studied smectic liquid crystal in the past few years. The sequence of the smectic phases in this system is as follows (T in ° C):

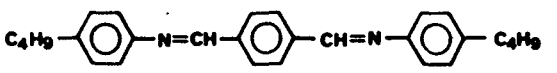

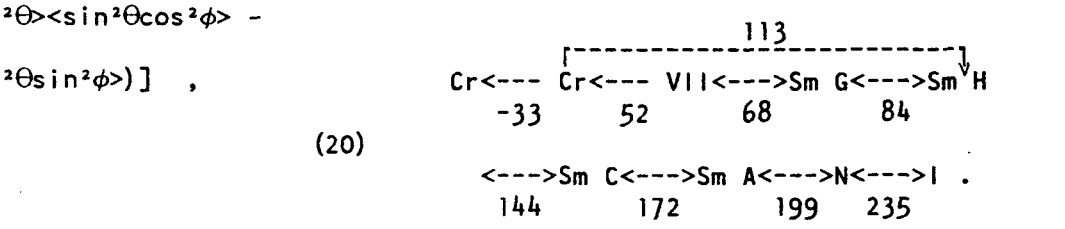

TBBA possesses two equivalent nitrogen nuclei in the central part of the molecule, so that the conclusions drawn from ^{14}N NQR data will concern the orientational ordering of the central molecular part or more precisely the ordering of C-CH=N-C linkage group. As it is exactly the ordering of the C=N electric dipoles in the linkage group which is of prime importance in the microscopic theory of the smectic phases, ^{14}N is an excellent probe for this study. The ordering of the molecular tails will not be discussed at

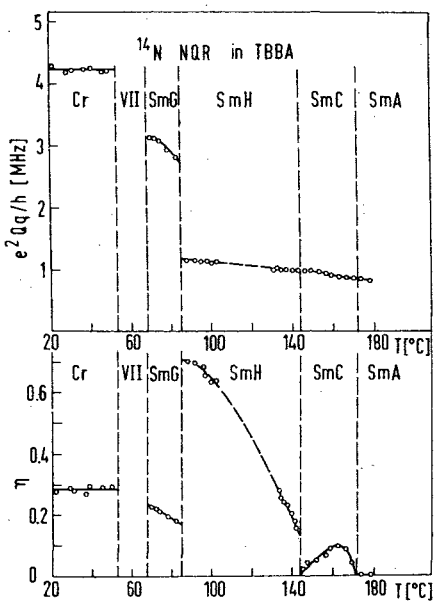

Figure 9. Temperature dependence of the ^{14}N quadrupole coupling constant e^2qQ/h and asymmetry parameter η in the smectic and crystalline phases of TBBA.

present.

The measurements of e^2qQ/h and η in TBBA (48-50) are presented in Figure 9. It can be seen that η is zero in the uniaxial smectic A phase. It is small, but non zero, in the Sm C phase and exhibits a maximum in the middle of this phase. On going to the Sm H phase, η discontinuously increases and reaches a very high value of about 0.7 at the low temperature end of this phase. Proceeding to the smectic G phase η abruptly decreases to about 0.18, and then slowly increases with decreasing temperature. In the solid phase the value of η is 0.28 and is practically temperature independent.

The quadrupole coupling constant shows a completely different temperature behavior. It increases slowly and continuously with decreasing temperature throughout the Sm A, Sm C and Sm H phases. On going to the Sm G phase, e^2qQ/h discontinuously increases by nearly 300%. In spite of this huge jump the value of e^2qQ/h at the end of the Sm G phase (3.28 MHz) is still significantly smaller than in the solid (4.22 MHz), demonstrating that motional averaging is still present. In the solid state the quadrupole coupling constant and η are temperature independent over the range +50° to -20° C, showing that the orientational order is complete.

A comprehensive analysis of the experimental data in the Sm C, Sm H and Sm G phases shows that the measured values of e^2qQ/h and η and in particular the large and temperature dependent value of η in the Sm H phase, are not compatible with either free rotation of the molecule around its long axis or polar ordering where one position would be preferred. The data are consistent with a bipolar ordering with $\langle\cos 2\psi\rangle \neq 0$, $\langle\cos\psi\rangle = 0$, $\langle\sin\psi\rangle = 0$, $\langle\sin 2\psi\rangle = 0$. The physical model for such motion, which is in agreement with NQR (48-50) and neutron scattering data (52), is as follows. The rigid "body" of the TBBA molecule is reorienting in a six-well potential around the long molecular axis. Four equilibrium sites are equivalent and have an occupation probability p_2 while the other two, separated by 180°, have a lower energy and an occupation probability $p_1 > p_2$. The bipolar order parameter is now given by

$$\langle\cos 2\psi\rangle = 2(p_1 - p_2), \qquad (21)$$
$$2p_1 + 4p_2 = 1 \ .$$

In addition to reorientations around

the long axis, fluctuations in the direction of the long axis also occur.

The degree of orientational ordering, which is given by the values of $\langle\cos 2\psi\rangle$ for ordering of the short molecular axis and by $\langle\cos\phi\rangle$ and S for ordering of the long molecular axis, increases from the high temperature smectic phases towards the solid crystalline state.

1. Smectic A Phase

The zero value of η in the Sm A phase shows that the molecules are freely rotating in this phase, or reorient between six equivalent potential wells around their long axes. The uniaxiality of the Sm A phase is thus not an "average" phenomenon but holds for each individual molecule. The fluctuations in the direction of the long axis are isotropic. Their magnitude $\langle\delta\Theta^2\rangle^{1/2} \simeq \langle\sin^2\delta\Theta\rangle^{1/2}$ can be straightforwardly determined from the quadrupole coupling constant through the relation

$$e^2qQ/h = (eqV_{z_0z_0}/h)\times [1 - (3/2)\langle\delta\Theta^2\rangle] \qquad (22)$$

which follows from equations 19 if it is taken into account that in the Sm A phase $\eta = 0$, $\langle\cos\phi\rangle = \langle\cos 2\phi\rangle = \langle\cos 2\psi\rangle = \langle\cos\psi\rangle = 0$, $\Theta_0 = 0$, and $\langle\delta\Theta^2\rangle \neq 0$. In TBBA the value of $V_{z_0z_0}$ equals 1.17 MHz in frequency units. This yields $\langle\delta\Theta^2\rangle^{1/2} \simeq 23°$ at 175° C corresponding to the nematic order parameter S = 0.75 for C-N=CH-C groups. This value is in excellent agreement with the results obtained from neutron scattering (52) and nuclear magnetic resonance experiments (18,52).

2. Smectic C Phase

In the biaxial Sm C phase the non-zero value of η demonstrates the occurrence of anisotropy in the molecular motion. A detailed analysis of e^2qQ/h and η shows that both partial rotational biasing of reorientations around the long axis and anisotropic fluctuations of this axis contribute to the non-zero value of η .

The degree of bipolar biasing is very small, the upper limit of $\langle\cos 2\psi\rangle$ being 0.005. This small value of the order parameter, though indicating a non-equivalency among the six-equilibrium positions, shows that the molecules still rotate nearly uniformly around their long axes (49).

The characteristic maximum in the temperature dependence of η shows that the orientational ordering of the long molecular axis in the Sm C phase is strongly perturbed by thermal agitation. The order parameters for the orientational ordering of the long molecular axis, $\langle\cos\phi\rangle$ and $S' = (1/2)\langle 3\cos^2(\Theta - \Theta_M) - 1\rangle$, which describes the polar fluctuations of the long molecular axis similarly as the "nematic order parameter" S (equation 1), have been calculated by assuming that (52):

(i) the Θ and ϕ motions are independent,

(ii) the ϕ distribution is of the form $g(\phi) \alpha \exp(\gamma'\cos\phi)$ (γ' describes the width of azimuthal fluctuations, i.e. the motion of long axes inside the smectic plane),

(iii) the Θ distribution is of the form $f(\Theta) \alpha \exp[\delta'\cos(\Theta - \Theta_M)]$ (Θ_M is the angle where the Θ distribution is peaked, δ' describes the width of the Θ distribution around Θ_M, i.e. the motion of the long axes outside the smectic plane),

(iv) the root mean square fluctuations in the polar angle $\langle\delta\Theta^2\rangle^{1/2} \simeq 22°$ are constant through the whole Sm C phase.

The results of this analysis are presented in Figure 10 (52). The temperature dependence of S', which increases from 0.75 at the Sm A → Sm C transition to 0.82 at the Sm C → Sm H transition, is mainly due to the temperature dependence of Θ_M. Θ_M increases in the Sm C phase with decreasing temperature similarly to the average tilt angle Θ_0. Fluctuations in the polar angle $\langle\delta\Theta^2\rangle^{1/2} \simeq 22°$ are

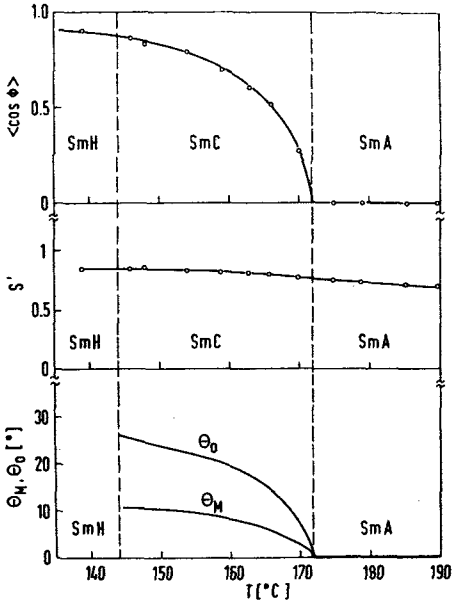

Figure 10. Temperature dependence of the azimuthal (<cosϕ>) and polar (S') fluctuations in the direction of the long molecular axis in the smectic phases of TBBA (52). The values of the average tilt angle Θ_0 and the tilt angle Θ_M, at which the Θ distribution is peaked, are plotted as well.

smaller than those in the azimuthal angle ϕ, where the root mean square fluctuation is of the order of ~60° at T = 165° C (<cosϕ> = 0.5) and ~30° at T = 145° C (<cosϕ> $\simeq$ 0.85).

3. Smectic H Phase

The large temperature variation in η and the small temperature variation in e^2qQ/h in this phase demonstrate a significant bipolar biasing of the rotation around the long molecular axis. The six potential wells for this reorientation, which are compatible with the X-ray structure (12), are not all equivalent. Equations 16 with r = 4.49, which have been deduced for the case of uniaxial rotation with bipolar biasing without any fluctuations in the direction of the long molecular axis (S = 1), are already a rather good approximation to the experimental data (50). The calculated values of the bipolar order parameter <cos2ψ> vary from 0.03 at T = 140° C to 0.16 at the low temperature end of the Sm H phase (Figure 11). For <cos2ψ> $\simeq$ 0.1, the occupation

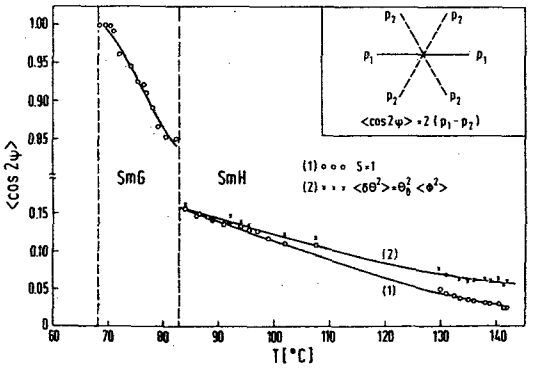

Figure 11. Temperature dependence of the bipolar orientational order parameter (<cos 2ψ>) in the Sm G and Sm H phases of TBBA. The values (1) have been calculated under the assumption of rigid long molecular axes, and (2) if the fluctuations in the direction of the long molecular axis are taken into account as well.

probability of each of the two low energy sites is p_1 = 0.2 whereas the occupation probability of each of the four high energy sites is p_2 = 0.15. Occupancy of the two preferred potential wells is thus about 30% more probable than that of the other four. It should be pointed out that neutron quasielastic scattering and X-ray data cannot discriminate between such small bipolar biasing and a uniform rotation model. Thus NQR, where the rotational bias is expressed in terms of a splitting frequency, provided the first direct evidence for biasing of the

uniaxial rotation of the central part of the TBBA molecules in the biaxial smectic phases.

The slight change (~20%) of e^2qQ/h in the Sm H phase indicates that fluctuations in the direction of the long axis are still present. If they are taken into account in the analysis (50) of the experimental data, the calculated values of $\langle\cos 2\psi\rangle$ are somewhat, though not significantly, higher at the high temperature part of the Sm H phase (Figure 11). The corresponding fluctuations in the direction of the long axis, which have been assumed to be roughly isotropic, range from ~15° close to the Sm C phase down to only ~2° at the boundary of the Sm G phase, where they freeze out completely.

4. Smectic G Phase

In the smectic G phase the ordering of the long molecular axis is perfect and the averaging of the EFG tensor is entirely due to the molecular reorientations around its long axis. The huge discontinuity in both e^2qQ/h and η at the Sm H → Sm G transition shows that the direction of the largest principal axis of the EFG tensor has changed due to the large increase of the bipolar biasing. It is not anymore parallel to the axis of reorientation. The value of $\langle\cos 2\psi\rangle$ calculated from equations 17 with $r = 4.49$ is already as high as 0.85 at the high temperature end of the Sm G phase and increases to 1 at the low temperature end (50). The four high energy states in the sixfold potential well are now nearly empty as $p_2 = 0.02$ at 82.5° C and $p_2 = 7 \times 10^{-3}$ at 72° C, whereas p_1 approaches 0.5. The molecular motion in the Sm G phase can be thus indeed described as 180° orientational jumps of the central part of the TBBA molecule.

5. Solid Crystalline Phase

On going from the Sm G to Sm VII and further to the crystalline phase, the 180° jumps freeze out so that $\langle\cos\psi\rangle = \langle\cos 2\psi\rangle = 1$ and $\langle\sin\psi\rangle = \langle\sin 2\psi\rangle = 0$. The freeze out of the 180° jumps probably happens in the Sm VII phase where no measurements could be made because the proton T_1 is too short.

In the crystalline solid phase the C-N=CH-C groups are already completely rigid, as demonstrated by the fact that neither the ^{14}N quadrupole coupling constant nor the ^{14}N asymmetry parameter vary with temperature. The EFG tensor in the molecular frame is (49,50):

$$(eQV_{ij}/h)\ (\text{MHz}) = \begin{pmatrix} -3.15 & \pm 0.15 & \pm 2.41 \\ \pm 0.15 & 1.98 & \pm 0.40 \\ \pm 2.41 & \pm 0.40 & 1.17 \end{pmatrix}.$$

B. Chiral Smectic TBACA

The central part of the chemical structure of terephtal-bis-amino-methyl- butyl cinnamate (TBACA) is the same as that of TBBA. The tails contain the asymmetric carbon which is responsible for the chirality and optical activity of this substance in its right- and left-handed optically active forms. In the vicinity of the chiral group is the strongly polar -COO group. The sequence of phase transitions in TBACA, first reported by Urbach and Billard (53), is the following (T in ° C):

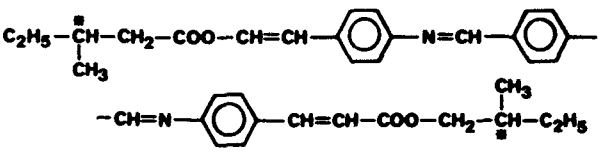

$$\underset{}{Cr_1} \overset{130}{\longrightarrow} Sm\ H^* \ (Cr_2) \overset{149}{\longrightarrow} Sm\ C^* \overset{180}{\longrightarrow} Sm\ A \overset{242}{\longrightarrow} N \overset{288}{\longrightarrow} I\ .$$

The structure of the various mesophases of TBACA has not yet been determined by X-ray crystallography as this has been done for TBBA. Electron-diffraction studies and NQR data (39,54) show that the phase Cr_2 is a liquid crystalline phase, most probably the Sm H* phase. Thus this name will be used for the

smectic phase obtained by cooling from the Sm C* phase.

The temperature dependence of e^2qQ/h and η of both equivalent nitrogens in the central part of TBACA (49) is presented in Figure 12 for the Sm A, Sm C*

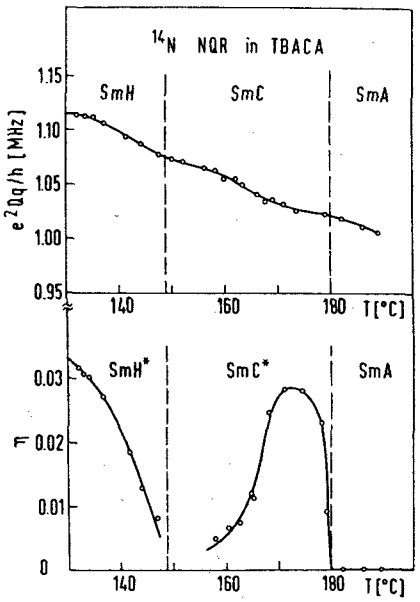

Figure 12. Temperature dependence of the ^{14}N quadrupole coupling constant e^2qQ/h and asymmetry parameter η in the smectic phases of TBACA.

and Sm H* phases. The ^{14}N quadrupole coupling constant slowly increases with decreasing temperature without showing any discontinuities at the Sm A → Sm C* or Sm C* → Sm H* transitions. The values of η in the Sm H* phase of TBACA are less than one tenth of these in TBBA.

The proton spin-lattice relaxation time in the solid phase of TBACA is too short to allow a determination of the double-resonance spectra. This makes the analysis of the ^{14}N NQR data in TBACA more difficult than in TBBA as the rigid lattice V_{ij} tensor in the molecular frame cannot be determined. However, it should not be appreciably different from that determined for TBBA as the central parts of both molecules are the same. In the following we shall assume that V_{ij} is the same in both TBACA and TBBA. The same holds for the magnitude of the tilt angle Θ_0.

In view of these approximations, the analysis of the ^{14}N data in TBACA is more tentative than in TBBA. We further assume that the Θ and ϕ motions are independent and that the magnitude of fluctuations in the long molecular axis is small enough to allow the expansion of sine and cosine of $\delta\Theta$ and ϕ in a power series with two or three terms. Thus one is able to determine the values of the order parameters $\langle\cos\psi\rangle$ or $\langle\cos 2\psi\rangle$, as well as the magnitude of the mean square fluctuations in the long molecular axis $\langle\delta\Theta^2\rangle$ and $\langle\phi^2\rangle$ (41).

1. Smectic A Phase

The value of η is zero in the Sm A phase of TBACA as in TBBA. The uniaxial rotation around the long molecular axis and the "nematic" fluctuations in the direction of this axis are isotropic.

2. Smectic C* Phase

The value of η is smaller than in TBBA but non-zero. The occurrence of a maximum in the temperature dependence of η indicates that the anisotropy in molecular motion is produced mainly by anisotropic fluctuations in the direction of long molecular axes. If the orientational ordering of the short molecular axes is neglected, $\langle\delta\Theta^2\rangle^{1/2}$ and $\langle\phi^2\rangle^{1/2}$ can be calculated at each temperature. In Figure 13 they are plotted for $V_{z_0z_0} = 1.15$ MHz. The fluctuations in the azimuthal angle are larger than in the polar angle throughout the smectic C* phase. The root mean square value of the polar fluctuations, $\langle\delta\Theta^2\rangle^{1/2}$, increases slowly from ~10° close to the boundary between the Sm H* and the Sm C* phase to ~15° at the Sm C* → Sm A transition. This value is in good agreement with that calculated from e^2qQ/h at the boundary between the Sm C* and Sm A phase (where $\langle\cos\phi\rangle = \langle\cos\psi\rangle = \langle\cos 2\psi\rangle = 0$),

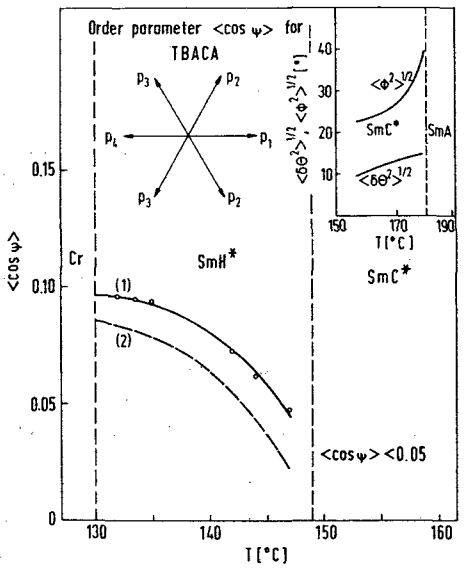

Figure 13. The temperature dependence of the polar order parameter $\langle\cos\psi\rangle$ and of the fluctuations in the direction of the long molecular axis ($\langle\delta\Theta^2\rangle^{1/2}$ and $\langle\phi^2\rangle^{1/2}$) in the Sm C* and Sm H* phases of TBACA (full line represents the calculated values of $\langle\cos\psi\rangle$ for V_{ZoZo} = 1.08 MHz and the broken line for V_{ZoZo} = 1.15 MHz).

which turns out to be 15.5°. The fluctuations in the azimuthal angle, $\langle\phi^2\rangle^{1/2}$, increase rapidly in the Sm C* phase and diverge as the Sm A phase boundary is approached.

On the basis of the NQR data in the Sm C* phase it is not possible to say whether or not the rotation around the long axis in the Sm C* phase of TBACA is biased. Nevertheless the biasing should be polar and very small, in accordance with the conclusions drawn for the Sm H* phase. Its upper limit is estimated as $\langle\cos\psi\rangle < 0.02$.

3. Smectic H* Phase

The NQR data in the Sm H* phase (54) can be explained by polar biasing of the uniaxial rotation around the long molecular axis with $\langle\cos\psi\rangle \neq 0$ and $\langle\cos2\psi\rangle \simeq 0$. If, on the other hand, bipolar ordering with only $\langle\cos2\psi\rangle \neq 0$ or a uniform rotation around the long molecular axis is assumed, no physically reasonable solution which would agree with the experimental data can be obtained. The physical model for polar ordering is that the molecule reorients around the long axis in a sixfold potential which is biased due to the coupling of the rotatable electric dipole with the local electric field. Due to coupling of the dipole to the local electric field ($-\mu E$) the six orientations are nonequivalent, with

$$p_i \propto (1/6)\exp[\mu E(\cos\psi_i)/kT]. \qquad (23)$$

For such a set of probabilities $\langle\cos\psi\rangle \neq 0$, while $\langle\cos2\psi\rangle \ll \langle\cos\psi\rangle$ if the coupling term is smaller than kT.

The temperature dependence of the polar order parameter $\langle\cos\psi\rangle$ in the Sm H* phase is shown in Figure 13. The $\langle\cos\psi\rangle$ values have been calculated for two different values of V_{ZoZo} : 1.15 MHz and 1.08 MHz. The higher value is close to that determined for TBBA (see above), and the lower one is the lowest which still gives reasonable solutions. In the whole Sm H* phase the values of $\langle\cos\psi\rangle$ are small, ranging from ~0.1 at the low temperature end to ~0.02 at the high temperature end of this phase. For $\langle\cos\psi\rangle = 0.07$ the difference in the probabilities between the most favorable position ($p_1 = 0.19$) and the least favorable position ($p_2 = 0.14$) is thus only ~30%. In the chiral Sm H* phase of TBACA the polar biasing of the molecular rotation around its long axis is thus rather weak. This is compatible with the small value of the spontaneous polarization observed in ferroelectric liquid crystals (39).

The accompanying fluctuations in the direction of the long molecular axis are smaller than 10°. They can be ignored and the experimental data explained by polar ordering only.

C. The Smectic B Phase of IBPBAC

The above results have shown that in

the two dimensional translationally ordered biaxial smectic phases of TBBA and TBACA the tilting of the molecules is associated with a biasing of the molecular rotation around the long axis. To establish whether this relation is general we investigated the orientational ordering of the short molecular axes in the untilted two dimensional translationally ordered Sm B phase of isobutyl-4-(4'-phenylbenzylideneamino)-cinnamate (IBPBAC). The sequence of the smectic phases in this system is as follows (T in ° C) (55):

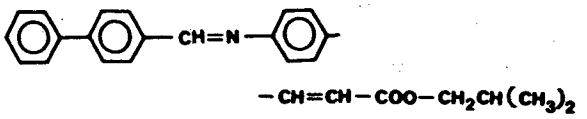

86 114 162
Cr <----> Sm E <----> Sm B <---->

206 214
Sm A <----> N <----> I .

The ^{14}N quadrupole coupling constant in the Sm B phase of IBPBAC (1.11 MHz at 137° C and 1.09 MHz at 146° C) (56) is comparable to the values found in TBBA, whereas the value of the asymmetry parameter is much smaller ($\lesssim 0.015$ at 137° C and ~ 0 at 146° C). This demonstrates that the rotation around the long molecular axis is practically "free" in the Sm B phase, i.e. the molecules seem to reorient between 6 equivalent sites in a hexagonally packed structure. The fluctuations in the direction of the long molecular axis ($\langle \delta\Theta^2 \rangle^{1/2}$) are estimated to ~12° at 140° C.

The above results show that there is indeed a close relation between the molecular tilt and the biasing of molecular rotation around the long axes in two dimensional ordered smectic systems. Biasing is polar in tilted chiral systems, bipolar in tilted achiral systems, and absent in untilted systems.

D. $(C_{10}H_{21}NH_3)_2CdCl_4$: A Lipid Bilayer Embedded in a Crystalline Matrix

The occurrence of phase transitions in cell membranes (57,58) has recently attracted a great deal of attention. It has been convincingly demonstrated (61,62) that the transitions in living cell membranes are due exclusively to the lipid component of the bilayer membrane. Most phase transition studies have therefore been performed on model lipid membranes, which are similar in their structural properties to biomembranes but can be better characterized physically and exhibit sharper phase transitions. Lipid bilayers of dipalmitoyl phosphatidyl choline (DPPC) exhibit two first-order phase transitions (63), the main transition at T_{c_2} = 42° C connected with a melting of the chains, and the pretransition at T_{c_1} = 33° C. Most model lipid membranes are difficult to obtain in a single crystalline form. This is however not the case with $(C_{10}H_{21}NH_3)_2CdCl_4$ (abbreviated as C10Cd), the hydrocarbon part of which represents a smectic lipid bilayer exhibiting two structural phase transitions at T_{c_1} = 35° C and T_{c_2} = 39° C in analogy to biomembranes.

The projection of the structure of C10Cd on the b-c plane at room temperature is shown in Figure 14. The structure consists of $CdCl_4^{2-}$ layers sandwiched between well ordered alkylammonium chains which are tilted by 40° with respect to the normal to the layer. The ammonium end of each chain is linked to the layer by N-H···Cl hydrogen bonds, and each chain is coordinated by six others. The entropy change at the lower phase transition T_{c_1}, $(0.9 \pm 0.3)R$ per mole chains, can be explained by an order-disorder transition of rigid chains between two equivalent sites. However, the entropy change at the higher phase transition T_{c_2} corresponds to 0.8 R per R-C-C-R bond and can be explained only by a "melting" of the chains, or what is equivalent, by rapid chain isomerization via kink diffusion.

^{14}N quadrupole resonance data show that on going from the low temperature to the intermediate phase the polar-NH_3 groups and the alkyl chains start flipping by 90° around their chain axes, so that neighboring chains move in opposite directions as in a two-dimensional

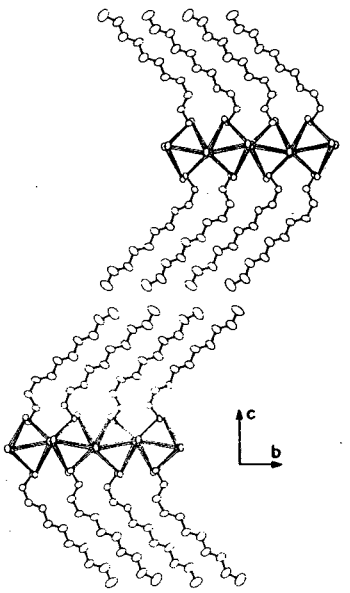

Figure 14. Projection of the structure of C10Cd on the b-c plane at room temperature.

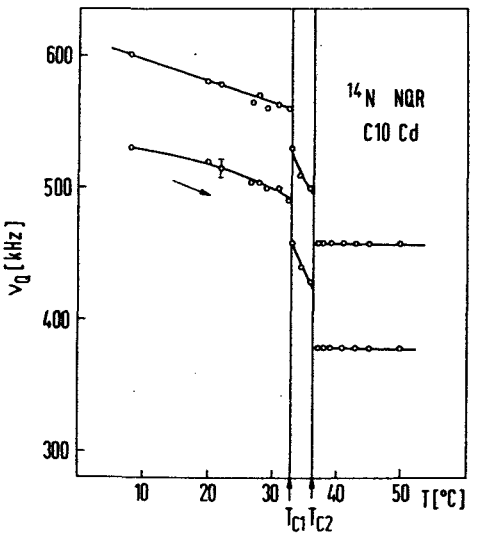

Figure 15. Temperature dependence of the ^{14}N NQR frequencies in C10Cd.

array of connected gears (64,65).

As the motion of the ammonium polar heads between the two equilibrium sites, characterized with ^{14}N EFG tensors T(1) and T(2), is fast on the NQR time scale, the observed ^{14}N NQR spectrum is determined by the time averaged EFG tensor:

$$\langle T(t)\rangle = (1/2)[1 + p]T(1) + (1/2)[1 - p]T(2) \quad . \qquad (24)$$

Here p is the orientational order parameter for the 90° flipping of the alkyl-ammonium chains. As T(1) and T(2) are known from single crystal experiments at low temperature in the completely ordered phase, the temperature dependence of p = p(T) can be determined from the observed temperature dependence of the NQR frequencies (Figure 15). The results are presented in Figure 16. In the low temperature phase p decreases from about 1 at T = 10° C towards zero as T_{c_1} is approached. In the intermediate and the high temperature phases p = 0, indicating that in these two phases the polar heads are disordered between two equilibrium sites.

The average orientation of the hydrocarbon chains and their degree of melting has been determined by ^{13}C NMR. In the intermediate phase the chains are still tilted and relatively rigid whereas in the high temperature phase they are on average normal to the smectic layers. The transition to the high temperature phase is also connected with a significant decrease in the nematic order parameter S of the alkyl chains though S is non-zero even in the high temperature phase.

The hydrocarbon part of C10Cd thus represents a smectic liquid crystal with a structure similar to the interior of the bilayer lipid membranes. We shall therefore try to

describe (64,65) the two phase transitions in ClOCd by a Landau type expansion of the non-equilibrium free energy F in terms of order parameters Θ_0, $S - S_c$ and p, used in the theory of smectic liquid crystals:

$$\begin{aligned} F = {} & (1/2)A\Theta_0^2 + (1/4)B\Theta_0^4 \\ & + e(T - T_{c_2})(S - S_c) \\ & - (1/2)c(S - S_c)^2 + (1/4)d(S - S_c)^4 \\ & + (1/2)ap^2 \\ & + (1/4)bp^4 - (1/2)A'\Theta_0^2(S - S_c) \\ & - (1/2)a'p^2(S - S_c) \quad . \end{aligned} \tag{25}$$

Here S stands for the average nematic order parameter and A, B, e, c, d, a, b, A' and a' are all positive constants. The Sm C order parameter Θ_0 gives the average tilt of the molecules with respect to the layer normal, whereas p is the orientational order parameter for the 90° flipping of the chains and the terminal NH_3 groups between the two equilibrium orientations corresponding to $p = \pm 1$. S_c is the critical value of the average nematic order parameter S, i.e. the arithmetic average of S in the melted and rigid phases coexisting at the first-order transition temperature T_{c_2} (Figure 16). In deriving equation 25 we assumed that the melting of the chains is the important driving mechanism which induces the transitions in S as well as in Θ_0 and p. It should be noted that here S is, in contrast to the isotropic-nematic transition, not a symmetry breaking order parameter and is different from zero both above and below T_{c_2}. Therefore the linear term in the expansion of F in powers of $(S - S_c)$ is not equal to zero, as in the case of nematic liquid crystals, but has the same structure as the free energy at liquid-gas phase transitions.

Minimizing the total free energy with respect to p, Θ_0 and S we obtain the following stable solutions:

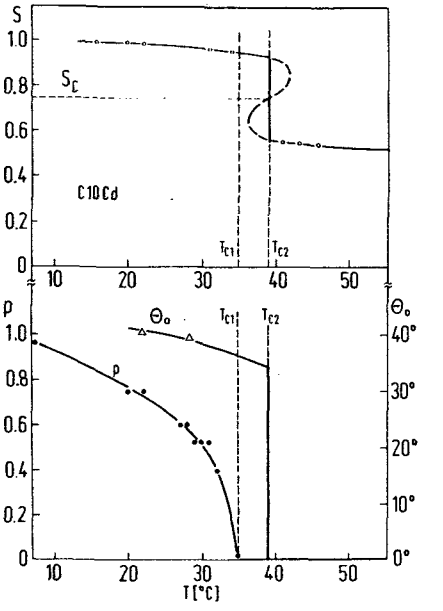

Figure 16. Comparison between the calculated and the observed temperature dependences of the order parameters S, p and Θ_0 for ClOCd.

$$\begin{aligned} T > T_{c_2} &: S < S_c,\ \Theta_0 = 0,\ p = 0\ , \\ T_{c_1} < T < T_{c_2} &: S > S_c,\ \Theta_0 \neq 0,\ p = 0 \\ T < T_{c_1} &: S > S_c,\ \Theta_0 \neq 0,\ p \neq 0. \end{aligned} \tag{26}$$

The high temperature transition at T_{c_2} corresponds to a partial melting of the chains which simultaneously destroys the tilting of the molecules, whereas the low temperature transition at T_{c_1} corresponds to an orientational transition and a disordering of the polar "heads". The temperature dependence of the order parameters S, Θ_0 and p is shown in Figure 16 together with the experimental values determined in this study.

NOTE:This review covers the field until April 1980 when it was submitted for publication. Revised May, 1983.

REFERENCES

[1]P. G. de Gennes, The Physics of Liquid Crystals, Oxford University Press, London, 1974.

[2]M. H. Stephen, J. P. Straley, Rev. Mod. Phys. 46, 618 (1974).

[3]S. Chandrasekhar, Rep. Progress Phys. 39, 615 (1976).

[4]G. W. Gray, in Molecular Structure and Properties of Liquid Crystals, Academic Press, New York, 1962.

[5]H. Sackmann and D. Demus, Mol. Cryst. Liq. Cryst. 2, 81 (1966).

[6]H. Sackmann, J. Phys. Coll. C3 40, 5 (1979).

[7]A. de Vries, Mol. Cryst. Liq. Cryst. 24, 337 (1973).

[8]A. de Vries, Liquid Crystals, Pramana Suppl. Indian Academy of Sciences, Bangalore, 1975, p. 93.

[9]A. de Vries, A. Ekachai, and N. Spielberg, J. Phys. Coll. C3 40, 147 (1979).

[10]J. Doucet, A. M. Levelut, and M. Lambert, Phys. Rev. Lett. 32, 301 (1974).

[11]J. Doucet, A. M. Levelut, M. Lambert, L. Liebert, and L. Strzelecki, J. Phys. Coll. C1 36, 13 (1975).

[12]A. M. Levelut, J. Phys. Coll. C3 37, 51 (1976).

[13]A. J. Leadbetter, J. Frost, J. P. Gaughan, and M. A. Masid, J. Phys. Coll. C3 40, 185 (1979).

[14]A. J. Leadbetter and P. G. Wrighton, J. Phys. Coll. C3 40, 234 (1979).

[15]J. D. Litster, J. Als-Nielsen, R. J. Birgeneau, S. S. Dana, D. Davidov, F. Garcia-Golding, M. Kaplan, C. R. Safinya, and R. Schaetzing, J. Phys. Coll. C3 40, 339 (1975).

[16]J. W. Doane, Magnetic Resonance of Phase Transitions, Academic Press, New York 1979, p. 172.

[17]R. A. Wise, D. H. Smith, and J. W. Doane, Phys. Rev. Ser. A 7, 1366 (1973).

[18]Z. Luz, R. C. Hewitt, and J. J. Meiboom, J. Chem. Phys. 61, 1758 (1974).

[19]B. Deloche, J. Charvolin, L. Liebert, and L. Strzelecki, J. Phys. Coll. C1 36, 21 (1975).

[20]G. J. Krueger, H. Spiesecke, and R. Van Steenwinkel, J. Phys. Coll. C3 37, 123 (1976).

[21]R. Blinc, M. Vilfan, M. Luzar, J. Seliger, and V. Žagar, J. Chem. Phys. 68, 303 (1978).

[22]H. Hervet, F. Volino, A. J. Dianoux, and R. E. Leckner, Phys. Rev. Lett. 34, 451 (1975).

[23]F. Volino, A. J. Dianoux, and H. Hervet, J. Phys. Coll. C3 37, 55 (1976).

[24]A. J. Leadbetter, R. M. Richardson, and C. J. Carlile, J. Phys. Coll. C3 37, 65 (1976).

[25]H. M. Conrad, H. H. Stiller, C. G. B. Frischkorn, and G. Shirane, Sol. Stat. Commun. 23, 571 (1977).

[26]J. Doucet, M. Lambert, A. M. Levelut, P. Porquet, and B. Dorner, J. Physique 39, 173 (1978).

[27]J. J. Benattar, A. M. Levelut, L. Liebert, and F. Moussa, J. Phys. Coll. C3 40, 115 (1979).

[28]W. Helfrich, J. Phys. Coll. C3 40, 105 (1979).

[29]J. Doucet, P. Keller, A. M. Levelut, and P. Porquet, J. Physique 39, 548 (1978).

[30]W. L. McMillan, Phys. Rev. Ser. A 4, 1238 (1971).

[31]W. L. McMillan, Phys. Rev. Ser. A 8, 1921 (1973).

[32]R. J. Meyer and W. L. McMillan Phys. Rev. Ser. A 9, 899 (1974).

[33]R. J. Meyer, Phys. Rev. Ser. A 13, 1613 (1976).

[34]A. Wulf, Phys. Rev. Ser. A 11, 365 (1975).

[35]A. Wulf, J. Chem. Phys. 63, 1564 (1975).

[36]R. G. Priest, J. Chem. Phys. 65, 408 (1976).

[37]D. Cabib and L. Benguigui, J. Physique 38, 419 (1977).

[38]B. W. van der Meer and G. Vertogen, J. Phys. Coll. C3 40, 222 (1979).

[39]R. B. Meyer, L. Liebert, L. Strzelecki, and P. Keller, J. Physique Lett. 36, 69 (1975).

[40]R. Blinc, Phys. Stat. Sol. Ser. B 70, K29 (1975).

[41]R. Blinc and B. Žekš, Phys. Rev. Ser. A 18, 740 (1978).

[42]R. Blinc and F. C. de Sa Barreto, Phys. Stat. Sol. Ser. B 87, K105 (1978).

[43]S. R. Hartman and E. L. Hahn, Phys. Rev. 128, 2042 (1962).

[44]F. M. Lurie and C. P. Slichter,

Phys. Rev. 133, 1108 (1964).
[45]D. T. Edmonds, Bull. Magn. Reson., in press.
[46]A. Abragam, The Principles of Nuclear Magnetism, Oxford University Press, London, 1961.
[47]J. Seliger, R. Osredkar, M. Mali, and R. Blinc, J. Chem. Phys. 65, 2887 (1976).
[48]J. Seliger, R. Osredkar, V. Žagar, and R. Blinc, Phys. Rev. Lett. 38, 411 (1977).
[49]J. Seliger, V. Žagar, and R. Blinc, Phys. Rev. Ser. A 17, 1149 (1978).
[50]R. Blinc, J. Seliger, M. Vilfan, and V. Žagar, J. Chem. Phys. 70, 773 (1979).
[51]D. W. Allender and J. W. Doane, Phys. Rev. Ser. A 17, 1177 (1978).
[52]A. J. Dianoux and F. Volino, J. Physique 40, 181 (1979).
[53]W. Z. Urbach and J. Billard, C. R. Acad. Sci. (Paris) Ser. B 274, 1287 (1972).
[54]M. Vilfan, R. Blinc, J. Seliger, and V. Žagar, Ferroelectrics 24, 211 (1980).
[55]A. J. Leadbetter, R. M. Richardson, and J. C. Frost, J. Phys. Coll. C3 40, 125 (1979).
[56]M. Vilfan, J. Seliger, V. Žagar, and R. Blinc, Phys. Lett. 79A, 186 (1980).
[57]D. Chapman, Quant. Rev. Biophys. 8, 185 (1975).
[58]J. F. Nagle, J. Membr. Biol. 27, 233 (1976).
[59]J. F. Nagle, J. Chem. Phys. 58, 252 (1973).
[60]J. F. Nagle, Proc. R. Soc. London, Ser. A 337, 569 (1974).
[61]D. L. Melchior and J. M. Stein, Biochim. Biophys. Acta 466, 148 (1977).
[62]S. Marčelja, Biochim. Biophys. Acta 367, 165 (1974).
[63]E.Sackmann, Ber. Buns. Phys. Chem. 82, 891 (1978).
[64]R. Blinc, M. I. Burgar, V. Rutar, B. Žekš, R. Kind, H. Arend, and G. Chapuis, Phys. Rev. Lett. 43, 1679 (1979).
[65]R. Kind, S. Pleško, H. Arend, R. Blinc, B. Žekš, J. Seliger, B. Ložar, A. Levstik, C. Filipič, V. Žagar, G. Lahajnar, F. Milia, and G. Chapuis, J. Chem. Phys. 71, 2118 (1979).